Biomedicine & Pharmacotherapy 196 (2026) 119043

Contents lists available at ScienceDirect

Biomedicine & Pharmacotherapy

journal homepage: www.elsevier.com/locate/biopha

Nanodiscs embedded with μ-opioid receptors as decoy receptors to reverse opioid overdose

Jin Yoo [a,1], Hanhee Cho [b,c,1], Heewon Yang [d], Jinseong Kim [b], Seung Hwan Lee [e], Kwangmeyung Kim [b,f,*], Tai Hyun Park [a,d,**]

[a] School of Chemical and Biological Engineering, Institute of Chemical Processes, Seoul National University, Seoul 08826, Republic of Korea
[b] Graduate School of Pharmaceutical Sciences, College of Pharmacy, Ewha Womans University, Seoul 03760, Republic of Korea
[c] Noxpharm Co., LTD., Seoul 03759, Republic of Korea
[d] Nutritional Science & Food Management, Ewha Womans University, Seoul 03760, Republic of Korea
[e] Department of Bionano Engineering, Center for Bionano Intelligence Education and Research, Hanyang University, Ansan 15588, Republic of Korea
[f] Graduate Program in Innovative Biomaterials Convergence, Ewha Womans University, Seoul 03760, Republic of Korea

ARTICLE INFO

Keywords:
Fentanyl overdose
Acute withdrawal
Decoy receptor
Nanodisc
μ-opioid receptor
Opioid inhibition
Blood-brain barrier

Opioid overdose, particularly involving synthetic opioids such as fentanyl, has emerged as a critical public health crisis worldwide. Fentanyl possesses significantly higher potency than traditional opioids such as morphine or heroin, leading to a dramatic increase in opioid-related mortality [1,2]. It is now a key driver of the overdose crisis, with a majority of synthetic opioid–related deaths in the U.S. attributed to illicit fentanyl and its analogs. Moreover, fentanyl's hidden presence in counterfeit medications significantly heightens the risk of fatal overdoses among users who may be unaware of its inclusion. The current standard of care for opioid overdose is the administration of naloxone, a μ-opioid receptor (μOR) antagonist that rapidly reverses respiratory depression by displacing opioids from their receptors [3,4]. However, naloxone directly binds to the orthosteric site of μOR, abruptly blocking receptor signaling. This mechanism can induce severe acute withdrawal symptoms, including anxiety, agitation, and autonomic instability, especially in individuals with established opioid dependence [5–7]. Importantly, such direct antagonism may promote receptor desensitization and internalization, thereby reducing long-term treatment efficacy with repeated use [8,9]. Recent neuroscientific studies have revealed that fentanyl addiction is mediated by dual reinforcement circuits [10]. While μOR activation in the reward circuit promotes dopamine release, withdrawal-associated dysphoria is driven by μOR activity in the central amygdala. Although naloxone does not activate μOR signaling directly, abrupt antagonism of μOR disrupts opioid-dependent neural homeostasis. Recent studies have shown that sudden μOR blockade can indirectly engage aversion-related circuits, particularly within the central amygdala, thereby precipitating dysphoria and withdrawal-associated negative affect [11,12].

To overcome these limitations, we propose μOR-embedded nanodiscs (μOR-NDs) as decoy receptors that sequester opioids with native receptor affinity, enabling opioid neutralization without direct orthosteric antagonism. A decoy receptor is a strategy that involves a receptor-like structure designed to selectively capture disease-related ligands or drugs, thereby neutralizing their biological activity [13,14]. Decoy receptors have been widely investigated as a therapeutic strategy due to their ability to selectively sequester pathogenic ligands without triggering downstream signaling, thereby enabling targeted neutralization with minimal off-target effects and reduced toxicity. Unlike

* Corresponding author at: Graduate School of Pharmaceutical Sciences, College of Pharmacy, Ewha Womans University, Seoul 03760, Republic of Korea.
** Corresponding author at: Nutritional Science & Food Management, Ewha Womans University, Seoul 03760, Republic of Korea.
E-mail addresses: kimkm@ewha.ac.kr (K. Kim), thpark@ewha.ac.kr (T.H. Park).
[1] These authors contributed equally to this work.

https://doi.org/10.1016/j.biopha.2026.119043
Received 10 December 2025; Received in revised form 3 January 2026; Accepted 21 January 2026
Available online 11 February 2026

conventional decoy receptors that merely mimic receptor structure, μOR-ND incorporates fully functional μ-opioid receptors, enabling direct and selective binding of opioid molecules with native receptor affinity. The μOR is a key receptor mediating the effects of both endogenous opioids (e.g., β-endorphins, enkephalins, dynorphins) and exogenous opioids (e.g., morphine, fentanyl, codeine, heroin) [15,16]. Also, the nanodisc platform enables this functional reconstitution of receptor by offering a lipid bilayer environment that maintains the structural integrity and ligand-binding capability of μOR in a cell-free system [17, 18]. Conventional nanocarriers such as liposomes exhibit limitations including heterogeneity, instability, and difficulty in reconstituting full-length membrane proteins. In contrast, nanodiscs offer a homogeneous, stable, and protein-compatible platform, making them better suited for decoy receptor-based therapeutics [19–21].

Unlike conventional antagonists, μOR-ND does not interfere directly with receptor function but instead operate through a non-competitive, extracellular sequestration mechanism. This indirect mode of action represents a fundamentally different therapeutic approach from traditional antagonism-based strategies. Since μOR-ND does not interact with the orthosteric site of μOR in central nervous system, they avoid abrupt disruption of neural signaling and enable a gradual detoxification process. This approach contributes to minimizing acute withdrawal symptoms and reduces the risk of receptor desensitization.

In this study, we report the successful fabrication of nanodiscs embedded with fully functional μOR-ND. *In vitro* binding assays confirmed that μOR-ND selectively and effectively binds to fentanyl, a representative exogenous opioid, demonstrating preserved ligand recognition and native receptor activity. To evaluate their biocompatibility and targeting capability, we conducted pharmacokinetic, biodistribution, and *ex vivo* analyses. These studies revealed that μOR-ND exhibits favorable systemic stability and tissue distribution, with significant accumulation in the brain.

The observed significant accumulation within brain tissue suggests that μOR-ND may has the capacity to access the central nervous system (CNS). This property may be associated with the high-density lipoprotein (HDL)-like structural characteristics of nanodiscs, which are lipid–protein complexes, and is consistent with previous reports describing brain-associated distribution of HDL-based particles. However, the

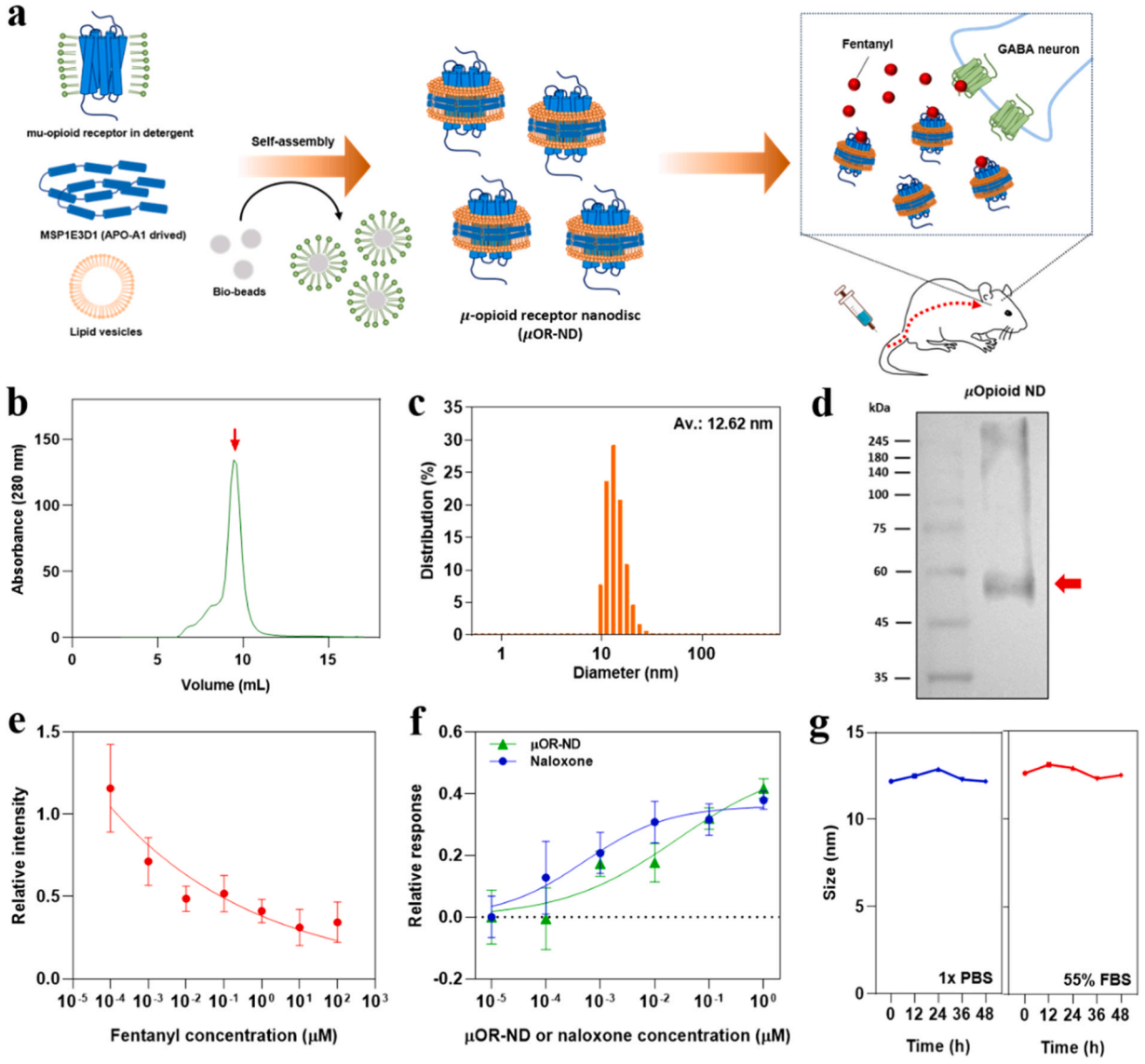

Fig. 1. Characterization of μOR-NDs. (a) Schematic diagram of μOR-ND production and purification. (b) Size-exclusion chromatography plots of μOR-ND after self-assembly process and (c) Size distribution of μOR-ND by dynamic light scattering (DLS) analysis. (d) Western blot analysis of μOR-ND using an anti-His antibody. (e) cAMP response in HEK-293T cells expressing μOR at various concentrations of fentanyl. (f) cAMP response in HEK-293T Cells expressing μOR at various concentrations of μOR-ND or naloxone. (g) Stability evaluation of μOR-ND in PBS and FBS.

molecular mechanisms underlying blood–brain barrier (BBB) transport were not directly elucidated in this study, and the observed brain distribution of μOR-ND may result from a combination of multiple in vivo transport processes. Nevertheless, the ability of μOR-ND to exert pharmacological effects associated with brain tissue without directly interfering with endogenous μOR signaling suggests that this platform holds potential for further development as a CNS–targeted therapeutic strategy.

1. Results and discussion

1.1. Characteristics of mu-opioid receptor-embedded nanodisc (μOR-ND)

μOR was expressed in *E. coli*, purified via affinity column chromatography, and reconstituted into lipid nanodiscs. μOR-ND was formed through a self-assembly process utilizing MSP1E3D1 and phospholipids (Fig. 1a). Due to the presence of a mixture of μOR-NDs, bare NDs, and aggregated NDs post-assembly, size-exclusion chromatography (SEC) was employed to isolate the μOR-NDs. The SEC results revealed a distinct elution peak corresponding to μOR-ND at a retention volume of approximately 9–10 mL after sample injection (Fig. 1b). Through an *E. coli*-based protein expression system, the receptor can be produced at high yields, and as shown in the SEC diagram, the nanodiscs exhibit excellent production efficiency. This demonstrates the feasibility of large-scale manufacturing for therapeutic development. Dynamic light scattering (DLS) analysis showed that OR-NDs exhibited a narrow and well-defined size distribution centered at approximately 12 nm (Fig. 1c). The sharpness of the DLS peak further demonstrated the uniformity of the μOR-NDs. Western blot analysis, utilizing an anti-His antibody and indicating MSP cleavage, confirmed the presence of μOR within the nanodiscs (Fig. 1d). These results collectively validate the successful synthesis of μOR-ND. In this study, we estimated that each μOR-ND incorporates approximately 1–2 μ-opioid receptors, based on the nanodisc diameter (~10 nm) and the average size of membrane receptors (~4 nm). Although the exact stoichiometry remains difficult to determine due to current limitations in nanodisc characterization techniques, we minimized non-functional particles by removing receptor-free nanodiscs during SEC purification.

To evaluate the functional equivalence of extracellularly produced μOR to that expressed in cells, an *in vitro* functionality assay was performed using fentanyl, a μOR agonist. The assay involved measuring cAMP-induced luciferase activity, with forskolin serving as a positive control. The results demonstrated a dose-dependent decrease in luciferase activity upon fentanyl treatment, consistent with μOR-mediated adenylate cyclase inhibition via the Gαi pathway (Fig. 1e). Additionally, the inhibitory effects of fentanyl were assessed using the antagonist naloxone and the decoy receptor μOR-ND, showing that increasing concentrations of these substances led to a recovery in luciferase activity (Fig. 1f). These findings suggest that extracellularly produced μOR-ND retains functional characteristics akin to cell-expressed μOR and can act as a decoy receptor. Also, the EC_{50} value of μOR-NDs was comparable to that of naloxone, suggesting efficient receptor–ligand interactions and functional receptor activity. The inhibitory effects observed were quantitatively comparable, as reflected by similar mean response values within experimental variability. According to previous reports, fentanyl binds to μ-opioid receptors with a K_D of approximately 1.3 nM, morphine and β-endorphin with values around 1–2 nM [22,23], while naloxone ranges from 0.2 nM to 3.9 nM [24,25]. Since our nanodiscs incorporate full-length functional μ-opioid receptors, they are expected to exhibit comparable binding affinities. This prediction is consistent with the results observed in cell-based experiments.

For stability assessment, μOR-ND samples were stored in 1x phosphate-buffered saline (PBS) at 4°C for 7 days and in 55 % fetal bovine serum (FBS) at 37°C for 48 h (Fig. 1g). The 1x PBS condition was designed to evaluate storage stability, while the 55 % FBS condition was intended to simulate *in vivo* blood stability, reflecting the typical serum ratio. Both conditions exhibited minimal changes in μOR-ND size, indicating robust storage stability and biostability.

1.2. In vivo biodistribution analysis of μOR-ND

It is well known that the therapeutic efficacy of brain-targeting drugs largely depends on their *in vivo* behavior after crossing the BBB. Considering the hypothesis that HDL can undergo receptor-mediated transcytosis via membrane scaffold proteins, we evaluated the biodistribution of μOR-ND *in vivo*. To minimize the potential for dye-induced artifacts in biodistribution analysis, Cy5.5 conjugation to μOR-ND was carefully controlled, and unbound dye was removed through desalting. Given the known biocompatibility of Cy5.5, we believe its influence on the in vivo distribution of μOR-ND is negligible. *In vivo* imaging data (Fig. 2a) showed that μOR-ND signals rapidly accumulated in the brain region over time following intravenous (IV) injection. Region of interest (ROI) analysis of the pharmacokinetic plots indicated that brain accumulation peaked at 0.5 h post-injection (Fig. S1). These results demonstrate that μOR-ND can quickly reach the brain through the bloodstream and effectively cross the BBB to enter the target region.

To more accurately observe the *in vivo* biodistribution of μOR-ND labeled with Cy5.5, major organ analysis was performed (Fig. S2). The analyzed organs included the liver, lungs, spleen, kidney, heart, and brain. Fluorescence analysis was conducted by extracting the organs 3 and 48 h after IV injection of the drug (Fig. 2b). Fig. 2c shows the fluorescence intensity for each organ. As expected, the highest fluorescence intensity was observed in the liver, which metabolizes μOR-ND, and fluorescence accumulation was also noted in the brain, the target site. Following the major organ analysis, *ex vivo* analysis was conducted to examine the time-dependent distribution of μOR-ND in the brain and kidneys in detail (Fig. 2d and S3). Fluorescence imaging of the brain revealed that μOR-ND is rapidly delivered to the brain and subsequently secreted over time (Fig. 2e). Fluorescence imaging of the kidneys indicated that μOR-ND exiting the brain is excreted through the kidneys, suggesting that μOR-ND can be effectively eliminated from the body without accumulation. Biodistribution and *ex vivo* imaging data indicate that μOR-ND undergo time-dependent clearance from the brain followed by renal elimination, suggesting that sequestered opioid molecules are cleared together with the nanodisc carrier. Within the duration of the present study, no evidence of opioid dissociation or re-entry into systemic circulation was observed; however, detailed long-term pharmacodynamic analyses will be required to fully characterize the fate of nanodisc-bound opioids.

Fig. S4 presents the biodistribution analysis results of μOR-ND in the blood. For comparison, μOR not structured into a nanodisc was used. The nanodisc platform, composed of phospholipids, demonstrated excellent lipophilicity in the blood and allowed for prolonged circulation. Pharmacokinetic (PK) analysis over time revealed that μOR-ND exhibited superior retention in the blood compared to μOR alone (Fig. S5). This suggests that the nanodisc platform not only serves to structure μOR but also provides a stable retention effect in the blood.

Further study is required to elucidate the mechanism of BBB passage during brain accumulation of μOR-ND, but the possibility can be linked to MSP1E3D1, a membrane scaffold protein (MSP) used in nanodisc synthesis. MSP1E3D1 is derived from apolipoprotein A-1, a scaffold protein involved in HDL transport. HDL in the brain is known to play a role in cholesterol metabolism, with the brain containing approximately 23 % of the total cholesterol in human body [26,27]. HDL has been implicated in brain cholesterol metabolism and has also been studied for its neuroprotective effects. Previous studies on the BBB crossing mechanism of HDL, particularly in lipid transport and utilization in the brain, suggest that scavenger receptors may mediate this process. The proposed “HDL hypothesis” is based on the structural and functional similarity between lipid nanodiscs and endogenous HDL. Nanodiscs are stabilized by membrane scaffold proteins derived from apolipoprotein

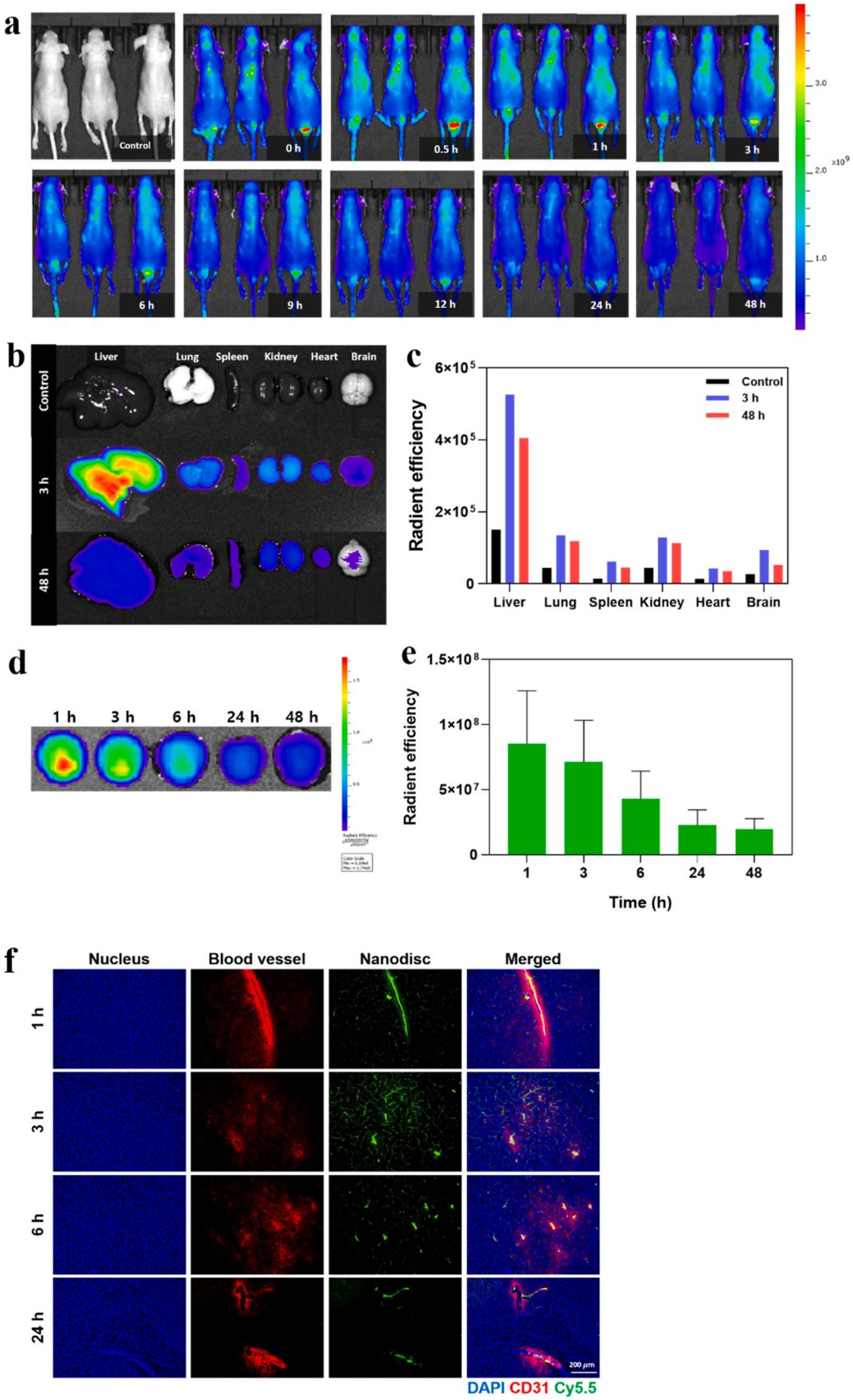

Fig. 2. *In vivo* biodistribution analysis of μOR-ND. (a) Biodistribution of μOR-ND *in vivo*: Fluorescence images of mice taken at different time points after IV injection of μOR-ND. (b) *Ex vivo* fluorescence images of major organs (liver, lung, spleen, kidney, heart, and brain) dissected 3 and 48 h after injection. (c) Fluorescence intensity based on fluorescence ROI in major organs. (d) *Ex vivo* fluorescence images of brain dissected 1, 3, 6, 24 and 48 h after injection. (e) Fluorescence intensity based on fluorescence ROI in brain. (f) Blood-brain barrier (BBB) permeability assay of μOR-ND.

A-1, a key component of HDL particles involved in μOR-ND transport. Previous studies have shown that HDL and apolipoprotein A-1–containing complexes can cross the blood–brain barrier via receptor-mediated transcytosis pathways [28]. Accordingly, we hypothesized that μOR-ND may exploit similar HDL-associated transport mechanisms to facilitate brain accumulation.

To verify this hypothesis, an *in vivo* BBB permeability assay was conducted (Fig. 2f). Following IV injection of μOR-ND, the brains were extracted at 1, 3, 6, and 24 h, and the nuclei of brain cells and brain blood vessels were stained to analyze the distribution of μOR-ND. The

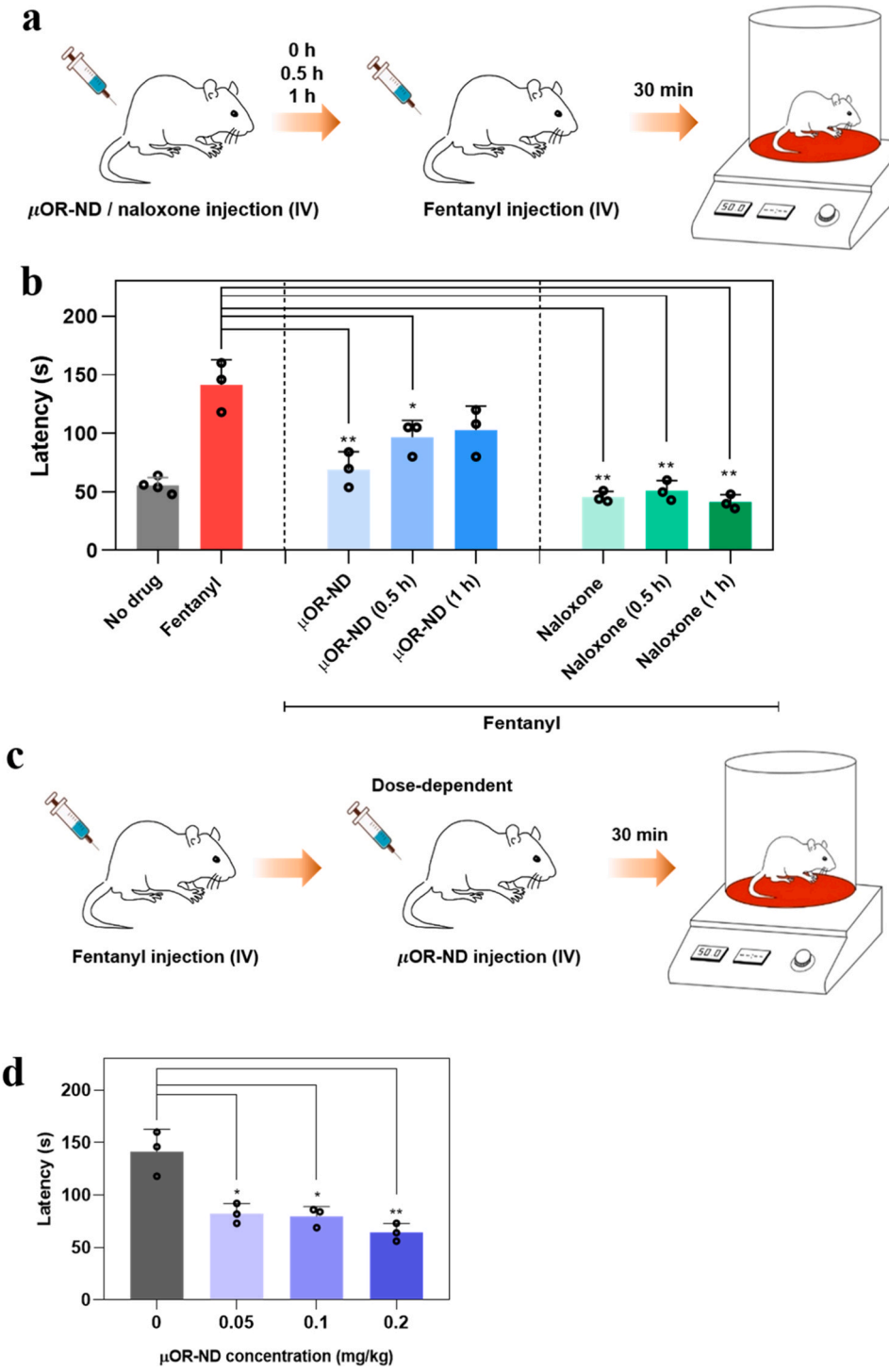

Fig. 3. Hot-plate analgesia assay. (a) Schematic diagram of hot-plate analgesia assay showing time-dependent efficacy results of μOR-ND and naloxone. (b) Results of the hot-plate analgesia assay when μOR-ND and naloxone were IV injected into mice at 0 h, 0.5 h, and 1 h intervals, respectively, followed by the injection of fentanyl at 20 ng/kg. Responses were measured as the latency to clear behavioral responses such as forepaw licking, hind paw licking, and escape attempts. (c) Schematic diagram of the hot-plate analgesia assay showing dose-dependent efficacy results of μOR -ND. (d) Results of hot-plate analgesia assay when μOR-ND was injected at concentrations of 0.05, 0.1, and 0.2 mg/kg immediately after IV injection of 20 ng/kg fentanyl into mice. Responses were measured as latency to clear behavioral responses such as forepaw licking, hind paw licking, and escape attempts. Bars represent mean values, and individual data points indicate measurements from independent animals (n = 3 per group).

analysis revealed that μOR-ND, which initially remained on the inner walls of blood vessels at 1 h, had significantly dispersed beyond the blood vessels into the brain regions by 3 h. While the fluorescence imaging results indicate accumulation of μOR-ND in the brain within 30 min post-injection, we acknowledge the limitations of this observation. The current imaging resolution does not allow clear differentiation between vascular-associated signals and deep parenchymal penetration. Additionally, potential dye leakage and background signal cannot be fully ruled out. Future studies employing high-resolution microscopy, radiolabeling, or quantitative mass spectrometry are warranted to precisely define the biodistribution and BBB permeability of the nanodiscs. Despite these limitations, our findings suggest a promising platform in biodistribution and BBB transport for further development.

Additionally, it was observed that μOR-ND gradually exited the brain over time. These fluorescence distribution results indicate that μOR-ND effectively crossed the BBB and permeated the brain extensively, demonstrating that the nanodisc can efficiently traverse the blood-brain barrier, similar to the delivery mechanism of HDL. Also, we analyzed the *in vivo* biodistribution of each component of the nanodisc. Fig. S6 shows the fluorescence signal after IV injection of each component of μOR-ND: μOR without refolding, μOR refolded in the form of a detergent micelle, MSP1E3D1, and bare nanodisc without a receptor. Fluorescence accumulation in the brain region was observed for MSP1E3D1 and bare nanodisc, confirming that MSP1E3D1 derived from Apolipoprotein A-1 facilitates BBB passage. Analysis of fluorescence intensity in the brain area revealed that the bare nanodisc form containing phospholipids accumulated a higher fluorescence signal than MSP1E3D1 alone, suggesting that the lipid-encased form of MSP is the most suitable for BBB passage. These results indicate that the lipid nanodisc form can be utilized as an effective means of targeting drugs for brain diseases by crossing the BBB.

1.3. *In vivo pharmacological efficacy analysis of μOR-ND*

We conducted a hot plate analgesia assay to verify whether μOR-ND effectively inhibits drug responses. Initially, to evaluate the efficacy of μOR-ND based on the timing of injection, μOR-ND was administered intravenously, followed by fentanyl (Fig. 3a). For comparison, a control experiment was performed using naloxone, a potent μOR inhibitor. Both μOR-ND and naloxone were administered at 0.1 mg/kg, with fentanyl also injected at 20 ng/kg.

Fig. 3b presents the latency in response after fentanyl injection at various time points following the administration of either μOR-ND or naloxone. Response latency was recorded until clear behavioral responses, such as forepaw licking, hind paw licking, and escape attempts, were observed, ensuring precise measurement. Ambiguous behaviors (e.g., raising hind or forepaws) were not included in the measurements. The results indicated that both μOR-ND and naloxone significantly reduced reaction times, confirming that μOR-ND effectively inhibited fentanyl in the brain.

Upon analyzing the results over time, the inhibitory effect diminished as time passed post-injection, aligning with prior *in vivo* biodistribution results. Additionally, while naloxone exhibited strong fentanyl inhibition, its direct antagonism of μOR in neurons often leads to severe opioid withdrawal symptoms, marked by intense pain and extreme withdrawal effects due to the rapid cessation of opioid activity. Hence, for narcotic treatment, a milder therapeutic approach might be preferred, potentially achieved through competitive inhibition via decoy receptors, as seen with the action mechanism of μOR-ND. Additionally, we aimed to optimize the dosage of μOR-ND to achieve effective drug inhibition. This experiment was designed to mimic real-usage conditions by first administering fentanyl, followed by three different doses of μOR-ND (Fig. 3c). Since naloxone is typically used for patients with acute opioid overdose, defined here as the acute pharmacological state induced by a single high-dose fentanyl administration, rather than chronic opioid dependence or addictive behavior, after the drug has already been administered, a similar approach was taken in this study. Although no statistically significant differences were observed among the tested doses, a non-significant trend toward greater recovery was noted at 0.2 mg/kg compared to the other concentrations (Fig. 3d). While the current study identifies 0.2 mg/kg as the most effective dose in vivo, future work will focus on comprehensive dose–response profiling to determine the ED50 value and define the therapeutic window with greater precision. This should be done considering not only the efficacy but also potential side effects.

Additionally, we aimed to compare the efficacy of μOR-ND and naloxone in inhibiting fentanyl through behavioral analysis of mice (Supplementary Video). For behavioral analysis, fentanyl was administered at a dose of 0.02 mg/kg, while μOR-ND and naloxone were used at doses of 0.1 mg/kg. Analysis of the behavioral video recordings revealed that control mice exhibited typical non-stereotypic behaviors (Supplementary Video 1). In contrast, mice administered fentanyl alone displayed excessive and persistent stereotypic behavioral patterns were observed following fentanyl administration, which are consistent with the proposed opioid sequestration hypothesis but do not, by themselves, define a specific underlying mechanism (Supplementary Video 2). However, co-administration (simultaneous administration) of fentanyl and μOR-ND resulted in a relative decrease in these stereotypic behaviors. The mice displayed non-stereotypic behaviors more similar to those of the control group (Supplementary Video 3), although further studies are required to examine whether this injection regimen induces other signs of withdrawal. This suggests that μOR-ND acts as a decoy receptor, inhibiting fentanyl's interaction with the μ-opioid receptor in neurons, thereby mitigating excessive opioid effects and promoting more typical behavioral patterns.

On the other hand, co-administration of fentanyl and naloxone led to a pronounced reduction in activity and controlled behavior, even more so than in the control mice, indicating the presence of acute opioid withdrawal symptoms induced by naloxone (Supplementary Video 4). While naloxone effectively blocks μ-opioid receptors in neurons and rapidly counteracts fentanyl's effects, it also precipitates severe withdrawal symptoms in mice.

In another experiment, we analyzed whether μOR-ND has therapeutic efficacy in treating fentanyl overdose. Currently, naloxone is used to rapidly revive overdose patients, and we sought to assess whether μOR-ND could serve a similar purpose. When mice were subjected to fentanyl overdose (0.1 mg/kg), they exhibited paralysis and ceased movement. Subsequently, μOR-ND and naloxone were administered at doses of 0.2 mg/kg, and recovery was evaluated (Supplementary Video 4). For differentiation, naloxone-treated mice were marked with red, while μOR-ND-treated mice were marked with blue. Behavioral analysis post-recovery revealed that red-marked mice recovered from paralysis but exhibited restricted behaviors, indicating acute opioid withdrawal symptoms induced by naloxone. In contrast, blue-marked mice recovered from paralysis and displayed behaviors comparable to normal, baseline mouse activity. Although our behavioral analysis demonstrated attenuated withdrawal responses following μOR-ND administration compared to naloxone, the absence of biochemical and physiological markers represents a limitation. Future studies incorporating serum corticosterone measurements, heart rate variability, and electrophysiological recordings will be essential to comprehensively characterize the therapeutic profile of μOR-ND in opioid withdrawal. Also, the supplementary videos are provided as qualitative visual references illustrating representative behavioral patterns following fentanyl administration and subsequent treatment. These observations are not intended to constitute quantitative behavioral analysis, and no statistical conclusions are drawn from the video data. More rigorous quantitative behavioral assessment will be an important focus of future studies to further elucidate these observations.

In conclusion, compared to naloxone, μOR-ND offers a significant advantage by providing mild inhibition that alleviates excessive opioid action without triggering acute withdrawal. Therefore, μOR-ND could

be a promising therapeutic strategy for safely mitigating the effects of fentanyl overdose while minimizing the risk of acute withdrawal symptoms.

1.4. *In vivo* biosafety analysis

The acute toxicity of μOR-ND was evaluated following *in vivo* administration to healthy mice. μOR-ND was IV injected at a dose of 0.1 mg/kg via the tail vein, and the mice were sacrificed 7 days post-injection to excise major organs, including the liver, lungs, spleen, kidneys, and heart. The excised organs were first sectioned and stained with hematoxylin and eosin (H&E) to investigate apoptotic cell death induced by the injected μOR-ND. Histological analysis revealed similar appearances between the control and treatment groups, with no obvious abnormalities, indicating no acute toxicity due to μOR-ND (Fig. 4a). In this study, histological analysis (H&E staining) of major peripheral organs was performed to evaluate systemic safety following single-dose administration. Although brain tissue was not included in the initial experiments, comprehensive histopathological analysis of the brain may be required to further assess neurological safety. The 7-day time point was selected based on standard protocols for evaluating acute or subacute toxicity following a single administration, and this study accordingly focused on assessing the safety of a single therapeutic dose. The current safety evaluation was conducted at the same dose as the efficacy study (0.2 mg/kg), but in future preclinical development, extended toxicological assessments including higher doses (10–100 ×) and repeated administrations will be necessary.

Additionally, a comprehensive serum chemistry panel was also assessed 7 days post-injection (Fig. 4b) to evaluate the short-term safety of μOR-ND through blood analysis. No significant changes were observed in the overall panel indices compared to normal mice, indicating no severe toxicity. However, levels of alkaline phosphatase (ALP), alanine aminotransferase (ALT); liver function parameters, total bilirubin (TBILI); a jaundice-related parameter and glucose (GLU) were lower compared to normal mice, suggesting that μOR-ND may have had some impact on appetite. Additional long-term studies are needed to investigate this further, but it is reassuring that no critical issues, such as a surge in liver function parameters due to toxicity, were observed. Overall, these data demonstrate that μOR-ND exhibits a favorable safety profile.

2. Conclusion

This study highlights the successful development of μOR-ND based on the concept of decoy receptors, presenting an innovative therapeutic strategy for central nervous system (CNS)-targeted opioid neutralization. A decoy receptor is designed to selectively capture pathological ligands without initiating intracellular signaling, thereby offering superior target specificity and safety compared to traditional antagonists. Unlike conventional mimetic constructs, μOR-ND incorporates fully functional endogenous receptor into the nanodisc platform, enabling the selective sequestration of exogenous opioids such as fentanyl.

Our findings demonstrate that μOR-ND effectively inhibits opioids as decoy receptors while avoiding the severe side effects commonly associated with traditional orthosteric antagonists such as naloxone [5,29]. Analytical characterization confirmed successful reconstitution of μOR into lipid-based nanodiscs, which maintained uniformity, stability, and structural integrity under various conditions. Although our μOR-ND demonstrated short-term stability in physiological buffers and serum, long-term storage stability (e.g., >7 days) and functional retention after lyophilization and reconstitution remain critical for clinical translation. Future studies should explore the physicochemical and functional integrity of μOR-NDs under storage and formulation conditions to ensure their viability as therapeutic agents.

A another finding of this study is the ability of μOR-ND to efficiently cross the BBB, as evidenced by rapid accumulation in the brain via in vivo biodistribution imaging. Although our *in vivo* imaging revealed notable brain accumulation of μOR-NDs, we recognize the importance of quantitative assessment (e.g., brain/plasma ratio) to further validate delivery efficiency. Future work will involve mass spectrometric or

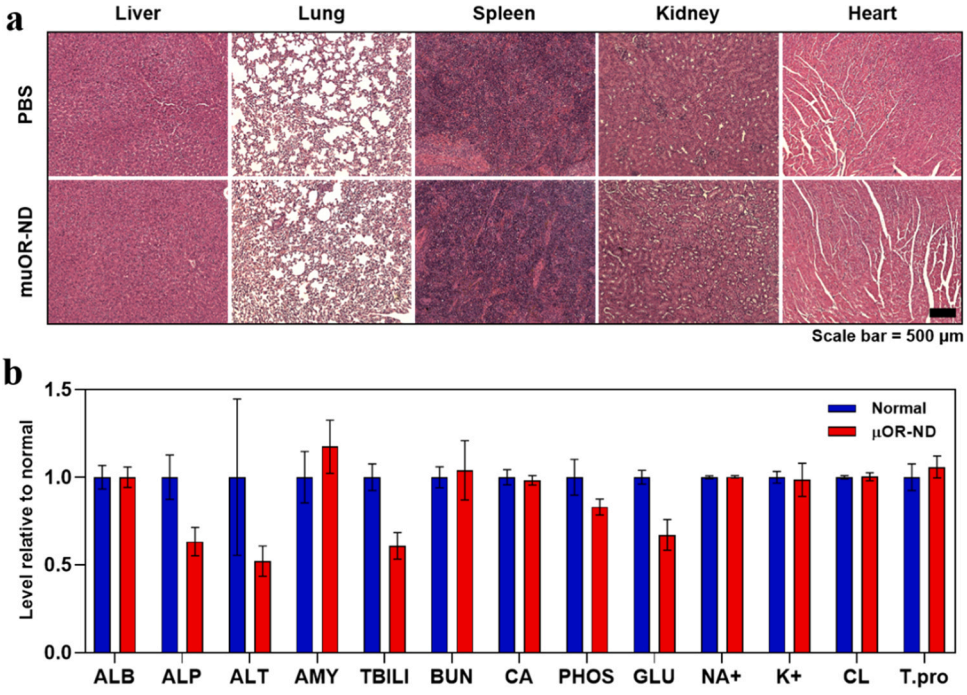

Fig. 4. *In vivo* biosafety of μOR-ND. (a) H&E staining of tissue sections of major organs (heart, liver, spleen, lung, kidney, and brain) 7 days after μOR-ND administration. Scale bar = 500μm. (b) Blood biochemistry panel analysis 7 days after μOR-ND administration. ALB, albumin; ALP, alkaline phosphatase; ALT, alanine transaminase; AMY, amylase; TBIL, total bilirubin; BUN, blood urea nitrogen; CA, calcium; PHOS, phosphorus; GLU, glucose; NA+ , sodium; K+ , potassium; TP, total protein; GLOP, globulin. n = 3 in all studies, and data are presented as mean+standard deviation.

radiolabel-based quantification to directly compare our platform with existing nanocarrier systems. This highlights the potential of nanodisc-based delivery systems for CNS-targeted therapies and their utility as carriers for therapeutic agents that require BBB penetration. While our study mentions the potential involvement of an HDL-like mechanism in nanodisc-mediated BBB penetration, we acknowledge that direct evidence for this pathway remains to be established. The core contribution of this work lies in demonstrating the therapeutic value and translational potential of decoy receptor-functionalized nanodiscs. Further investigation into the detailed mechanism of BBB transport—such as receptor-mediated transcytosis involving SR-B1—will be an important subject for future studies.

Biosafety evaluations in mice showed no observable toxicity, confirming the good tolerability of μOR-ND. In hot plate analgesia assays, μOR-ND significantly attenuated fentanyl-induced responses, in line with their biodistribution profiles. In contrast, naloxone caused severe withdrawal symptoms, while μOR-ND provided a gentler therapeutic effect through their decoy mechanism.

The development of μOR-ND is particularly timely in the context of the ongoing opioid crisis, which continues to cause devastating health and social consequences worldwide [1,30]. As fentanyl-related overdose deaths continue to rise, the need for safer and more effective therapeutic alternatives has become increasingly urgent. While naloxone remains a lifesaving drug, it is limited by its potential to induce withdrawal, receptor desensitization, and the need for repeated dosing. In contrast, μOR-ND function via a non-competitive, peripheral sequestration mechanism, bypassing central receptor blockade and thereby reducing adverse effects while preserving therapeutic efficacy. In this context, it is important to distinguish receptor-based decoy nanodiscs from other sequestration strategies, such as monoclonal antibody–based approaches. Monoclonal antibody–based sequestration strategies typically rely on ligand-specific recognition, limiting their applicability to predefined opioid structures. In contrast, μOR-ND leverages native receptor–ligand interactions, enabling class-wide sequestration of structurally diverse opioids while avoiding direct antagonism of neuronal μORs. Although antibody approaches may offer longer systemic half-lives, receptor-based nanodiscs provide a more versatile and physiologically compatible strategy for opioid neutralization.

Although naloxone exhibited better latency recovery in the later phase of the hot-plate analgesia test due to its high-affinity competitive antagonism at μ-opioid receptors, μOR-ND also induced rapid analgesic recovery in the early phase, even at low doses. Furthermore, mice treated with μOR-ND showed behavioral normalization comparable to untreated controls, suggesting that μOR-ND may alleviate opioid effects without triggering acute withdrawal symptoms. These findings support μOR-ND as a potential alternative to naloxone, offering a more balanced recovery with reduced side effects.

In summary, μOR-ND function as effective decoy receptors while also demonstrating the broader utility of nanodisc-based drug delivery platforms that can cross the BBB. The combination of these techniques represents a significant advance in the development of safer and more targeted treatment methods for CNS disorders, including opioid addiction. Given the urgency of the opioid epidemic, the introduction of such precision and less-side effect therapies is more critical than ever. Further research is needed to optimize dosing, evaluate long-term safety, and assess clinical applicability.

3. Methods

3.1. μOR production and purification

The production, solubilization, and purification techniques for *E. coli*-based G-protein coupled receptors (GPCRs) have been thoroughly studied in previous research [31].

The Rosetta™ 2 (DE3) *E. coli* strain (Merck, USA) was transformed with the pET-DEST42 vector containing the μOR genes. Following an overnight incubation at 37°C on LB agar plates with 100 μg/mL ampicillin, a colony was selected and cultured in 5 mL of LB medium with 100 μg/mL ampicillin for 6–7 h at 37°C and 200 rpm. This culture was then scaled up by inoculating 200 mL of LB medium containing 100 μg/mL ampicillin and incubating overnight at 37°C and 200 rpm. The 200 mL culture was transferred to 6 L of LB medium and grown at 37°C and 150 rpm until reaching an OD600 of 0.4–0.6.

Protein expression was induced with 1 mM IPTG for 4 h. Cells were harvested by centrifugation (4°C, 12,000 rpm, 10 min), and pellets were lysed via sonication in a buffer with 2 mM EDTA in 1X PBS. The sonication involved 5 cycles of 5 min each at 38 % amplitude and 4°C. The lysate was further concentrated by centrifugation (4°C, 12,000 rpm, 30 min) to obtain the insoluble fraction, which was solubilized overnight at 30°C in a buffer containing 20 mM SDS, 100 mM DTT, 1 mM EDTA, and 100 mM Tris Base (pH 8.0). After solubilization, the solution was centrifuged (25°C, 12,000 rpm, 30 min) and dialyzed using MEMBRA-CEL® dialysis membrane tubing (12–14 kDa cutoff) in a binding buffer (100 mM sodium phosphate, 10 mM SDS, pH 8.0). The μOR protein was purified with a HisTrap HP column (GE Healthcare, USA), washed with a buffer (100 mM sodium phosphate, 10 mM SDS, pH 7.0), and eluted with an elution buffer (100 mM sodium phosphate, 10 mM SDS, pH 6.0). The purified μOR protein was then exchanged into HEPES buffer I (20 mM HEPES, 25 mM cholate, 100 mM NaCl, pH 8.0) using a HiTrap Desalting column (GE Healthcare, USA) for subsequent nanodisc (ND) assembly.

3.2. μOR-ND assembly and purification

To simulate a native mammalian membrane environment, 1,2-dimyristoyl-sn-glycero-3-phosphocholine (DMPC) (Avanti Polar Lipids) was used. Lipids were dried from a chloroform solution using nitrogen gas and then placed under vacuum for 1 h to eliminate any residual chloroform. The dried lipids were resuspended in HEPES II buffer (20 mM HEPES, 100 mM NaCl, pH 8.0) to achieve a final lipid concentration of 24 mM. The purified μOR was added to the lipid solution, and the mixture was incubated on ice for 20 min. Subsequently, purified MSP1E3D1 was added, and the mixture was incubated at 25°C with gentle stirring for 2 h. The final concentrations in the mixture were 1 μM μOR protein, 3 μM MSP1E3D1, 390 μM lipids, and 25 mM cholate. To remove cholate, Bio-beads (Bio-Rad, USA) were added, and the mixture was incubated overnight at room temperature with mild shaking. After filtration through a 0.22 μm filter, the mixture was subjected to size exclusion chromatography (SEC) using a Superdex 200 Increase 10/300 GL column (Cytiva, USA) to separate unassembled and aggregated samples. The column was equilibrated with HEPES II buffer. 800 μL sample was loaded into the injection loop at a flow rate of 0.3 mL/min using an FPLC. Peaks corresponding to nanodiscs (ND) were collected and stored at −80°C until further analysis.

3.3. Characterization of OR nanodisc

For identification of μOR-ND, western blot analysis was performed. An acrylamide gel loaded with μOR-ND samples was transferred to nitrocellulose membrane and incubated overnight using anti-His antibodies after blocking process. Anti-mouse antibody was used for 2nd antibody treatment. Size distribution of μOR-ND were analyzed by dynamic light scattering (DLS) with a Zetasizer Ultra (Malvern Panalytical, England) under temperature of 25°C.

3.4. Inhibition of forskolin-based cAMP accumulation assays

1 × 105 cells of HEK-293T were transferred in a 96-well white-walled plate with DMEM and 5 % FBS medium. After overnight incubation, μOR and 22 F gene were co-transfected to HEK-293T cells for 48 h. For cAMP accumulation assay, 100 μL of HBSS buffer containing 2 % of Glosensor-cAMP reagent (Promega, USA) was added to each well

after removing the media by tapping. 10 μL of fentanyl was treated at each concentration into the assay wells, followed by 10 μL of 10 μM forskolin. Luminescence was measured for 30 min using Varioskan lux (Thermo Fisher, USA).

3.5. Biodistribution analysis of μOR-ND

To visualize the *in vivo* biodistribution of μOR-NDs, fluorescently labeled μOR-NDs were prepared by reacting the μOR-ND solution with Cy5.5 dye (Lumiprobe, USA) at a 1:10 molar ratio for 4 h at room temperature in the dark. Excess dye was removed via desalting with PBS buffer. Following a single IV injection of Cy5.5-labeled μOR-ND (0.1 mg/kg) into each mouse, the near-infrared fluorescence (NIRF) images of treated mice were captured at multiple time points (0, 0.5, 1, 3, 6, 9, and 12 h post-injection) using the IVIS Spectrum imaging system (PerkinElmer, USA). For ex vivo NIRF imaging, Cy5.5-labeled μOR-ND treated mice were sacrificed at each time point, and the five major organs, including the liver, lungs, spleen, kidneys, and heart, were excised. The excised organs were immediately imaged using the IVIS system. The fluorescence intensity of these organs was quantified using ImageJ software. All in vivo/ex vivo tests were performed according to the guidelines and regulations of the Institutional Animal Care and Use Committee (IACUC) at Ewha Womans University (approval no. EWHA IACUC 22–073–7)

3.6. Hot-plate analgesia assays

The hot plate was maintained at 55℃. To accurately measure responses, licking of the front or hind paws due to heat exposure and attempts to escape by jumping were considered responses [32,33]. To minimize tissue damage and burns, the mice were promptly removed from the hot plate after showing a reaction. Baseline responses were recorded before administering any substances. Response tests were conducted 30 min after the IV administration of each substance. To minimize the effect of fentanyl on the natural decomposition of the drugs, μOR-ND and naloxone were injected prior to fentanyl. Tests were conducted at various intervals to compare the inhibition effect of fentanyl based on the timing of μOR-ND and naloxone injections. Additionally, the effect of different doses of μOR-ND was assessed by administering fentanyl initially, followed by μOR-ND.

3.7. Biosafety analysis of μOR-ND

Blood biochemical panel analysis was performed by extracting approximately 2 mL of blood from the heart 7 days after IV injection of μOR-ND. The list of biochemicals used as a panel includes albumin (ALB), alkaline phosphatase (ALP), alanine aminotransferase (ALT), amylase (AMY), total bilirubin (TBIL), blood urea nitrogen (BUN), calcium (CA), and phosphorus (PHOS), glutamine (GLU), sodium (Na^+), potassium (K^+), total protein (TP), and globulin (GLOB).

Histological analysis was conducted by harvesting the heart, liver, spleen, lung, kidney, and brain from mice seven days post μOR-ND injection. As a control, a separate group was injected with PBS. Each organ was sectioned and stained with H&E for evaluation.

CRediT authorship contribution statement

Hanhee Cho: Writing – original draft, Resources, Methodology, Formal analysis. **Jin Yoo:** Writing – original draft, Validation, Investigation, Formal analysis, Conceptualization. **Kwangmeyung Kim:** Writing – review & editing, Supervision, Project administration, Methodology. **Seung Hwan Lee:** Writing – review & editing, Validation, Resources. **Jinseong Kim:** Resources, Investigation, Data curation. **Heewon Yang:** Validation, Investigation, Formal analysis. **Tai Hyun Park:** Writing – review & editing, Supervision, Project administration, Investigation, Funding acquisition.

Declaration of Competing Interest

The authors declare that they have no known competing financial interests or personal relationships that could have appeared to influence the work reported in this paper.

Acknowledgements

This study was supported by the Technology Innovation Program (25450828, Development of AI-based receptor and biosensor international standards) funded by the Ministry of Trade, Industry & Energy (MOTIE), Republic of Korea and supported by the National Research Foundation of Korea (NRF) grant funded by the Korea goverment (MSIT) (RS-2025-23324010).

Appendix A. Supporting information

Supplementary data associated with this article can be found in the online version at doi:10.1016/j.biopha.2026.119043.

Data availability

Data will be made available on request.

References

[1] N. Dasgupta, L. Beletsky, D. Ciccarone, Opioid crisis: no easy fix to its social and economic determinants, Am. J. Public Health 108 (2) (2018) 182–186.
[2] K. Lutfy, Opioid Crisis—An Emphasis on Fentanyl Analogs, MDPI (2020) 485.
[3] H.K. Kim, L.S. Nelson, Reducing the harm of opioid overdose with the safe use of naloxone: a pharmacologic review, Expert Opin. Drug Saf. 14 (7) (2015) 1137–1146.
[4] D.P. Wermeling, Review of naloxone safety for opioid overdose: practical considerations for new technology and expanded public access, Ther. Adv. Drug Saf. 6 (1) (2015) 20–31.
[5] M. Olmo, J. González-Barboteo, D. Moreno-Alonso, E. Coma, G. Serrano, Acute opioid withdrawal syndrome from naloxone/naloxegol interaction, BMJ Support. Palliat. Care 11 (4) (2021) 408–410.
[6] R. Purssell, J. Godwin, J. Moe, J. Buxton, A. Crabtree, A. Kestler, C. DeWitt, F. Scheuermeyer, S. Erdelyi, R. Balshaw, Comparison of rates of opioid withdrawal symptoms and reversal of opioid toxicity in patients treated with two naloxone dosing regimens: a retrospective cohort study, Clin. Toxicol. 59 (1) (2021) 38–46.
[7] E.L. van Dorp, A. Yassen, A. Dahan, Naloxone treatment in opioid addiction: the risks and benefits, Expert Opin. Drug Saf. 6 (2) (2007) 125–132.
[8] E.C. Klaasse, A.P. IJzerman, W.J. de Grip, M.W. Beukers, Internalization and desensitization of adenosine receptors, Purinergic Signal. 4 (2008) 21–37.
[9] S. Arttamangkul, M. Torrecilla, K. Kobayashi, H. Okano, J.T. Williams, Separation of μ-opioid receptor desensitization and internalization: endogenous receptors in primary neuronal cultures, J. Neurosci. 26 (15) (2006) 4118–4125.
[10] F. Chaudun, L. Python, Y. Liu, A. Hiver, J. Cand, B.L. Kieffer, E. Valjent, C. Lüscher, Distinct μ-opioid ensembles trigger positive and negative fentanyl reinforcement, Nature 630 (8015) (2024) 141–148.
[11] G.C. Gregoriou, S.D. Patel, S. Pyne, B.L. Winters, E.E. Bagley, Opioid withdrawal abruptly disrupts amygdala circuit function by reducing peptide actions, J. Neurosci. 43 (10) (2023) 1668–1681.
[12] G.B. Kaplan, B.L. Thompson, Neuroplasticity of the extended amygdala in opioid withdrawal and prolonged opioid abstinence, Front. Pharmacol. 14 (2023) 1253736.
[13] C. Zoccali, G. Tripepi, V. Stel, E.L. Fu, F. Mallamaci, F. Dekker, K.J. Jager, Decoy receptors as biomarkers for exploring aetiology and designing new therapies, Clin. Kidney J. (2024) sfae222.
[14] A. Mantovani, M. Locati, A. Vecchi, S. Sozzani, P. Allavena, Decoy receptors: a strategy to regulate inflammatory cytokines and chemokines, Trends Immunol. 22 (6) (2001) 328–336.
[15] C. Contet, B.L. Kieffer, K. Befort, Mu opioid receptor: a gateway to drug addiction, Curr. Opin. Neurobiol. 14 (3) (2004) 370–378.
[16] Q.N. Vo, P. Mahinthichaichan, J. Shen, C.R. Ellis, How μ-opioid receptor recognizes fentanyl, Nat. Commun. 12 (1) (2021) 984.
[17] H. Yang, D. Kim, J. Kim, D. Moon, H.S. Song, M. Lee, S. Hong, T.H. Park, Nanodisc-based bioelectronic nose using olfactory receptor produced in Escherichia coli for the assessment of the death-associated odor cadaverine, ACS Nano 11 (12) (2017) 11847–11855.
[18] M. Son, J.Y. Lee, H.J. Ko, T.H. Park, Bioelectronic nose: an emerging tool for odor standardization, Trends Biotechnol. 35 (4) (2017) 301–307.
[19] I.G. Denisov, S.G. Sligar, Nanodiscs for the study of membrane proteins, Curr. Opin. Struct. Biol. 87 (2024) 102844.

[20] J. Hao, M. Ishihara, G. Rapenne, K. Yasuhara, Lipid nanodiscs spontaneously formed by an amphiphilic polymethacrylate derivative as an efficient nanocarrier for molecular delivery to intact cells, RSC Adv. 14 (9) (2024) 6127–6134.
[21] K.M. Padmanabha Das, W.M. Shih, G. Wagner, M.L. Nasr, Large nanodiscs: a potential game changer in structural biology of membrane protein complexes and virus entry, Front. Bioeng. Biotechnol. 8 (2020) 539.
[22] A. Ricarte, J.A. Dalton, J. Giraldo, Structural assessment of agonist efficacy in the μ-opioid receptor: morphine and fentanyl elicit different activation patterns, J. Chem. Inf. Model. 61 (3) (2021) 1251–1274.
[23] M.S. Ahmed, D.-h Zhou, A.G. Cavinato, D. Maulik, Opioid binding properties of the purified kappa receptor from human placenta, Life Sci. 44 (13) (1989) 861–871.
[24] L.C. Newman, D.R. Wallace, C.W. Stevens, Selective opioid agonist and antagonist competition for [3H]-naloxone binding in amphibian spinal cord, Brain Res. 884 (1-2) (2000) 184–191.
[25] M. Trøstheim, M. Eikemo, J. Haaker, J.J. Frost, S. Leknes, Opioid antagonism in humans: a primer on optimal dose and timing for central mu-opioid receptor blockade, Neuropsychopharmacology 48 (2) (2023) 299–307.
[26] M. Turri, C. Marchi, M.P. Adorni, L. Calabresi, F. Zimetti, Emerging role of HDL in brain cholesterol metabolism and neurodegenerative disorders, Biochim. Biophys. Acta (BBA) Mole. Cell Biol. Lipids 1867 (5) (2022) 159123.
[27] C. Vitali, C.L. Wellington, L. Calabresi, HDL and cholesterol handling in the brain, Cardiovasc. Res. 103 (3) (2014) 405–413.
[28] P. Zhu, L. Xiao, Y. Wang, Mechanisms of high-density lipoprotein in regulating blood-brain barrier function: insights and implications, Fluids Barriers CNS 22 (1) (2025) 113.
[29] N. Chhabra, S.E. Aks, Treatment of acute naloxone-precipitated opioid withdrawal with buprenorphine, Am. J. Emerg. Med. 38 (3) (2020).
[30] M.A. Chisholm-Burns, C.A. Spivey, E. Sherwin, J. Wheeler, K. Hohmeier, The opioid crisis: origins, trends, policies, and the roles of pharmacists, Am. J. Health Syst. Pharm. 76 (7) (2019) 424–435.
[31] H.S. Song, S.H. Lee, E.H. Oh, T.H. Park, Expression, solubilization and purification of a human olfactory receptor from Escherichia coli, Curr. Microbiol. 59 (2009) 309–314.
[32] R. Kumar, S.S. Singh, S.B. Ray, Nimodipine potentiates the analgesic effect of morphine in the rat hot-plate test: implications in the treatment of pain, Indian J. Anaesth. 55 (4) (2011) 413–416.
[33] I. Sora, N. Takahashi, M. Funada, H. Ujike, R.S. Revay, D.M. Donovan, L.L. Miner, G.R. Uhl, Opiate receptor knockout mice define μ receptor roles in endogenous nociceptive responses and morphine-induced analgesia, Proc. Natl. Acad. Sci. 94 (4) (1997) 1544–1549.